

Upper Airway Occlusion Detection Using a Novel Ultrasound Technique

Mohammad A. Al-Abed, *Member, IEEE*, Peter Antich, *Senior Member, IEEE*,
Donald E. Watenpugh, and Khosrow Behbehani, *Senior Member, IEEE*

Abstract — Obstructive sleep apnea/hypopnea Syndrome (OSAHS) is the most common form of Sleep Disordered Breathing (SDB) and it is estimated to affect approximately 15% of US adult population. In this paper, we report on the results of *in vivo* experiments of an ultrasonic device for the non-invasive detection of obstructive sleep apnea/hypopnea (OSAH). A description of the ultrasonic system used is presented, followed by the results of a full night sleep study. The findings show a significant difference in the spectral features extracted from the received ultrasonic waveform during apneic breathing, compared to the hyperventilation that follows. Therefore, the findings indicate the feasibility of developing an ultrasonic detection device for low cost diagnosis of SDB.

I. INTRODUCTION

OBSTRUCTIVE Sleep Apnea/Hypopnea Syndrome (OSAHS) is a sleep disorder, characterized by repetitive pharyngeal collapse. It has been recently reported that prevalence of untreated sleep apnea is approximately 15% of the United States adult population [1], heightening the necessity for more wide spread screening. Patients diagnosed with OSAHS have high incidence of obesity, and exhibit an increased risk of hypertension, stroke, and depression. An association between OSAHS and high morbidity and mortality due to cardiovascular and cerebrovascular causes has been established [1-4].

Obstructive apneas consist of complete occlusion of the airway at the pharynx, causing a cessation of airflow for ten seconds or more with continuing respiratory effort despite the occlusion. Hypopnea is manifested by a decrease of 50% or more in the airflow for ten seconds or more, due to the narrowing of the airway at the pharynx [5]. An average of five events or more in an hour of sleep is considered clinically significant, and therefore worthy of medical intervention. This average measurement is called the

Apnea/Hypopnea Index (AHI) [4].

Nocturnal polysomnography (NPSG) performed in accredited sleep laboratories is the gold standard for diagnosis of OSAHS. However, due to the cost of such test and lack of sleep laboratories in all areas, low cost, yet reliable methods for diagnosis of SDB are highly desired. The current methods that have been developed for diagnosis and large-scale screening for SDB have focused on markers of physiological responses associated with events of airway occlusion, such as sympathoexcitatory or cardiovascular reactions.

There are several advantages in using ultrasonic in detecting OSAHS: it is safe (non-ionizing radiation, no contrast agent), non-invasive, low cost, and portable [6]. We have reported in [7] and [8] the results of *in vitro* and *in vivo* characterization of ultrasonic sensors for the detection of occlusion in an upper airway, and have presented preliminary results on temporal features extracted from the ultrasonic waves.

In this paper, we report preliminary results of an *in vivo* study for the detection of airway occlusion during apnea/hypopnea events using the spectral features of the ultrasonic waves. The experiment, design, protocol, inclusion and exclusion criteria are presented, followed by the signal post process and statistical analysis.

II. METHODOLOGY

A. Ultrasonic Sensor Array Design and Fabrication

The design, fabrication, and *in vivo* characterization of the sensor arrays used in this study were reported in [8]. The design of the transducers followed an optimization process.

While the design focused on maximizing the transmitted and received energy through the neck, it needed to allow full night study without interrupting the patient's sleep. Constraints for the transducer design included the heterogeneity of the neck anatomical media, the neck curvature, and the location of the site of the occlusion [8]. Fig. 1 illustrates the ultrasonic sensors used in this study.

In order to achieve maximum acoustic energy penetration through the neck, a low frequency and large surface area transducer is ideal [9]. However, low frequency transducers are usually bulky ($f < 1\text{MHz}$). Hence, An array of seven low-Q disk piezoelectric, with a central frequency of 3MHz

Manuscript received March 29, 2012. This work was supported in part by a grant from the U.S. Department of Energy.

M. A. Al-Abed is an assistant professor with the Department of Biomedical Engineering, the Hashemite University, Zarqa, 13135 Jordan (phone:+96253903333 ext:4923; fax: +96253826348; e-mail: mohammad@hu.edu.jo).

P. Antich is professor and chair emeritus of the Radiology Department at the University of Texas Southwestern Medical Center in Dallas, Dallas TX 75390 USA (e-mail: Peter.Antich@UTSouthwestern.edu).

D. E. Watenpugh is a physiologist and sleep medicine specialist with Sleep Consultants, Inc., Fort Worth, TX, 76104 USA.

K. Behbehani is a professor and chair of the Department of Bioengineering Department, the University of Texas at Arlington, Arlington, TX 76010 USA (e-mail: kb@uta.edu).

was chosen for this design, and a radius of $a = 5\text{mm}$. The thickness of the PZT crystal is 0.58mm , for $f=3\text{MHz}$. The divergence half angle, θ_R , is 3.5° [8-9]. This is the angle that the main lobe is enclosed in. The smaller this angle is, the higher the transducer's directivity [9].



Fig. 1. The ultrasonic sensor arrays constructed for this research. Both (a) receiver and (b) transmitter arrays were constructed using PZT-5A piezoelectric material with brass backing. The arrays were housed in silicon rubber for handling and placement on the patient's neck during sleep studies.

The design considerations for the receiver transducers are similar to those for the transmitter [8]. However, in order to achieve maximum reception, these transducers need to be designed with a wider beam width to allow for normal and oblique incidence of the received ultrasonic waveform, to account for the curvature of the neck. Small size elements are desirable for this purpose. In order to meet these design requirements, rectangular transducers were designed with width $W = 4\text{mm}$, and height $H = 10\text{mm}$. The divergence half angle, φ_R , is found to be 2.7° along the H -axis. The divergence half angle along the W -axis, θ_R , is found to be 6.8° [8, 9].

B. Sensor Array Placement

The site of occlusion of the airway during obstructive sleep apnea events differs slightly, with intra- and inter-subject variations. However, most studies, irrespective of the technique used to localize the occlusion, indicate that the main site of occlusion is the oropharynx, sometimes with extension to the laryngopharynx [10]. Figure 2 shows the actual placement of the sensors on a patient's neck prior to the start of the sleep study.

The sensor arrays, housed in silicon rubber, were placed on the patient's neck, just below the ear lobe, and behind the jawbone. The skin-transducer interface acoustic mismatch is reduced using water-based Aquasonic 100 Gel (Parker Labs, Inc., Fairfield, NJ, USA). The transmitter and receiver arrays are placed opposite of each other on the patient's neck. Surgical tape was used to keep the silicon rubber in place.

C. Full Night Sleep Study

To test the ultrasonic transducer assembly for *in vivo* detection of airway occlusion during apnea, a protocol for full night sleep study at an accredited sleep lab was submitted to and approved by the local IRB committee [8]. The protocol calls for recruitment of patients previously diagnosed with SDB, but do not have other underlying neurological or physiological abnormalities, for a full night sleep (6-8 hours) at an accredited sleep lab (Sleep Consultants, Inc., Fort Worth, TX). A consent form was provided and signed by the volunteers. The patients underwent full NSPG, in simultaneously with the ultrasonic transducers placed on the patient's neck. The transducers are placed along the length of the neck below the earlobe and just behind the mandibular joint. The area covered by the transducers on either side of the neck is about $2.5\text{cm} \times 8.0\text{cm}$.

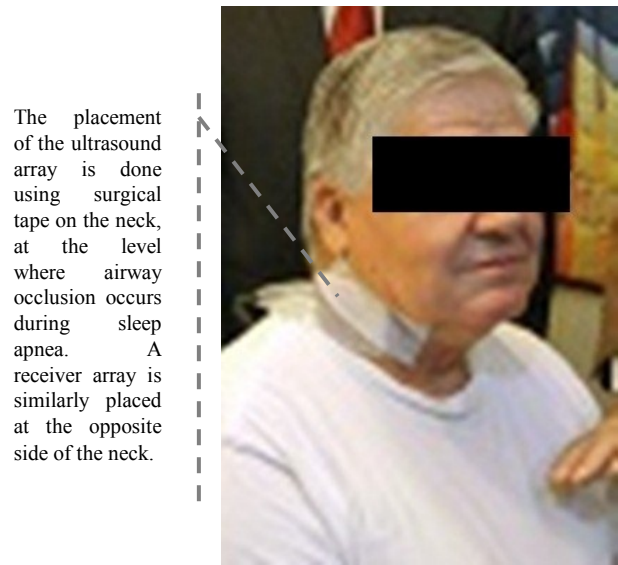


Fig. 2. This image illustrates the placement of the ultrasonic sensor array on the patient's neck just before the sleep study is conducted. A group of tandem physiological measurements is taken during the study to test and validate the feasibility of the design.

The data acquisition system used for the ultrasound experimental setup is described in [7-8]. The transmitters were simultaneously pulsed at 10 Pulse Repetition Frequency (PRF=10) using OmniScan[®] iX UT (Olympus NDT, Quebec, Canada). The transmitted and received signals from both transducer assemblies are acquired using Data Acquisition (DAQ) system (National Instruments NI PXI-5105, Austin, TX, USA) running at 30×10^6 Samples/s, 12-bits/Sample [8].

At the end of the study, a certified sleep expert, blind to the aims of this study, scored the NPSG data according to Rechtschaffen & Kales standard. The severity of SDB was measured using the apnea-hypopnea index (AHI).

D. Post Processing

Each second, there are 10 received pulses. The received signal is summed for each second into one waveform. This

waveform is then filtered using a Kaiser Window band-pass FIR filter ($f_L=0.15\text{MHz}$, $f_H=3.5\text{MHz}$, $N=100$, $\beta=0.05$) and rectified [11]. The peaks of the resultant signal are detected, and an envelope of the peaks is estimated using a cubic spline.

E. Waveform Envelope Feature Extraction

We calculated the spectral density of the envelope, and found that there are differences in the spectral distribution between respiratory event (RE) and hyperventilation breathing (HV). These differences are more evident in certain frequency bands than others. To quantify these differences, we integrated the area under the spectra in two frequency bands that appeared to have high variation in the spectral distribution between HV and RE.

1. The first band is a low frequency band and extends from 10-230 kHz. We define this band as the Very Low Frequency Envelope Spectral Band (VLSB).
2. Low Frequency Spectral Band (LSB)
A second band that appeared to have high variation in the spectral distribution between HV and RE is 230-487 kHz, and we define this band as Low Frequency Envelope Spectral Band (LSB).
3. High Frequency Spectral Band (HSB)
A third band that appeared to have high variation in the spectral distribution between HV and RE is 487-770 kHz, and we define this band as the High Frequency Envelope Spectral Band (HSB).
4. Very High Frequency Spectral Band (VHSB)
A fourth band that appeared to have high variation in the spectral distribution between HV and RE is 0.77-1.22 MHz, and we define this band as the Very High Frequency Envelope Spectral Band (VHSB). Figure 5.11 shows an illustration of these bands.

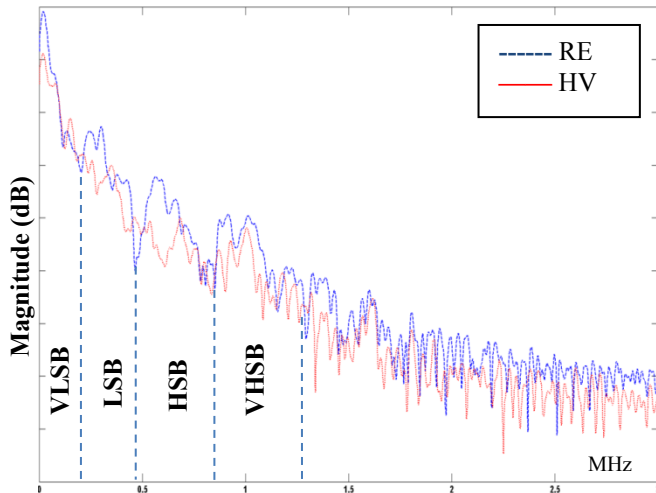


Fig. 3. An illustration of the method used to calculate the four Frequency Spectral Bands (VLSB, LSB, HSB, and VHSB). The power spectral density (PSD) of the envelope of the rectified signal is found using the Welch method (Hamming window, length = 500 points, 50% overlap). The LFSB is equal to the integration of the area under the curve between 10-230kHz, the LSB is equal to the integration of the area under the curve between 230-470kHz, the HSB is equal to the integration of the area under the curve between 470-770kHz whereas the HFSB is equal to the area under the curve between 0.77-1.22MHz. The x-axis is the frequency (0-3MHz), and the y-axis is in dB.

F. Respiratory Event Epoch Clipping

Each respiratory event (RE), whether it is apnea or hypopnea, is followed by a period of hyperventilation (HV). The aim is to quantify the changes in the received signal between RE and HV, using the spectral features extracted above. Each RE that is followed by 10 seconds of HV is clipped and considered for analysis.

The average spectral features for each RE can be calculated, and are denoted $\mu_{VLSB,n}^{RE}$, $\mu_{LSB,n}^{RE}$, $\mu_{HSB,n}^{RE}$ and $\mu_{VHSB,n}^{RE}$, respectively. The average spectral features for each HV that follows each RE can be calculated, and are denoted $\mu_{VLSB,n}^{HV}$, $\mu_{LSB,n}^{HV}$ and $\mu_{VHSB,n}^{HV}$, respectively. Notice that n denotes the index of the clipped epoch $1 \leq n \leq q$ where q is the total number of epochs used in the analysis.

G. Recruited Patient Demographics

One male volunteer was recruited (49 years old, BMI = 34.9 kg/m², AHI = 86.3). Duration of sleep study was 7 hours. There were $q=369$ epochs that met the criteria described above. From those, 197 were apnea events, and 172 hypopnea events. AHI).

H. Statistical Analysis

The ratio of the average of peaks in the HV period to the average of peaks in the RE for each epoch was calculated; that is, the ratio

$$R_{VLSB,n} = \mu_{VLSB,n}^{HV} / \mu_{VLSB,n}^{RE} \quad (1)$$

is found, where R_{VLSB} denotes Ratio of the spectral power between the respiratory event and the hyperventilation that follows it, calculated in the very low spectral band, defined in Section II.E. Similarly, three other ratios can be calculated for the remaining three features, as follows:

$$R_{LSB,n} = \mu_{LSB,n}^{HV} / \mu_{LSB,n}^{RE} \quad (2)$$

$$R_{HSB,n} = \mu_{HSB,n}^{HV} / \mu_{HSB,n}^{RE} \quad (3)$$

$$R_{VHSB,n} = \mu_{VHSB,n}^{HV} / \mu_{VHSB,n}^{RE} \quad (4)$$

The 95% confidence interval (CI) is calculated using the t -distribution as follows [12]:

$$R_{feature}^{CI} = \overline{R_{feature}} \pm (t_{0.05,q} \times \sigma_{feature} / \sqrt{q}) \quad (5)$$

where $\overline{R_{feature}}$ is the mean of four features calculated in Eqs. (1) - (4); $\sigma_{feature}$ is the standard deviation of these features; q is the number of epochs used ($q=197$ for apnea, $q=172$ for hypopnea, and $q=369$ for both combined); and $t_{0.05,q}$ is the two-tail critical t -value for a 95% confidence interval and q degrees of freedom (df). It is about 1.97 for the q values listed above.

III. RESULTS

The confidence interval for the epochs containing apnea, hypopnea, and the combination of both are plotted in Figure 4.

Notice that if the confidence interval does not include 1, it indicates that there is a significant difference between the average feature values between RE compared to the subsequent HV.

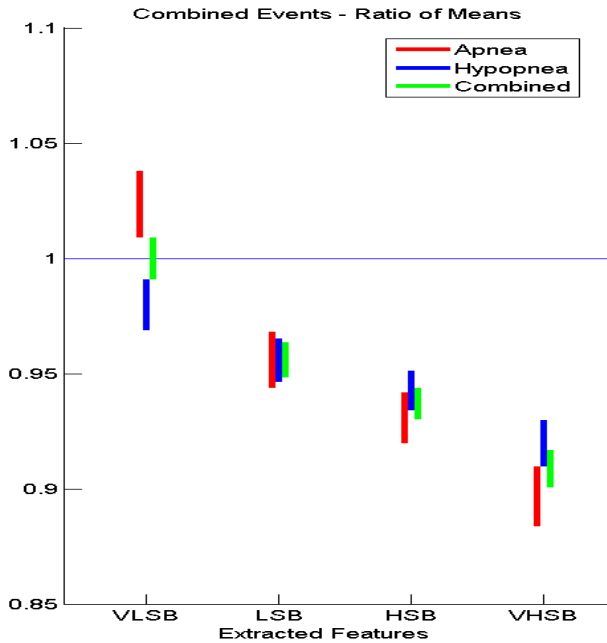


Fig. 4. The t -distribution 95%-Confidence Interval plots of the VLSB, LSB, HSB, VHSB for apnea and hypopnea epochs, and the combination of both epoch groups. HV/RE denotes the mean ratio of the average said feature between hyperventilation (HV) and the superseding respiratory event (RE).

IV. DISCUSSION

In this *in vivo* feasibility study for the use of ultrasonic pulses to detect the closure of the upper airway during apneic breathing, the ultrasonic transducer design followed a set of anatomical and practical considerations for overnight ultrasonic data acquisition.

Studying the epochs recorded using the ultrasonic transducers during the full night sleep study; we notice that spectral features extracted from these records show significant difference in the higher three frequency bands, namely LSB, HSB, and VHSB, while the VLSB does not show any change in the spectral energy when considering both apneic and hyponeic events combined.

Studying Fig. 4, and keeping in mind that these results are for the ratio of HV/RE, the results indicate higher spectral energy passing through the neck of the patient during apneic events compared to the energy levels during the hyperventilation period that follows. We can hypothesize the reason for such reduction in the HV/RE ration is that the occlusion of the airway during OSAH episodes reduces the acoustic energy loss in the ultrasonic beam pathway, due to the contact of the airway walls, and reduction of amount of air in the airway at the level of the ultrasonic beam.

V. CONCLUSION

This paper presented the spectral feature analysis of the *in vivo* study that the employs ultrasonic sensing for the non-

invasive detection of airway narrowing and occlusion. Using skin-mounted ultrasound transducer elements, an examination of the possibility of distinguishing apneic breathing from normal breathing was performed using epochs collected from one SDB volunteer. While the results presented here are preliminary, the use of ultrasound detection of airway occlusion events may offer a simple, cost effective, and specific screening tool for OSAHS breathing pattern.

VI. REFERENCES

- [1] T. Young, M. Palta, J. Dempsey, P. E. Peppard, F. J. Nieto, and K. M. Hla, "Burden of sleep apnea: rationale, design, and major findings of the Wisconsin Sleep Cohort study," *Wisconsin Medical Journal*, vol. 108, pp. 246-249, 2009.
- [2] P. J. Strollo and R. M. Rogers, "Obstructive Sleep Apnea," *New England Journal of Medicine*, vol. 334, pp. 99-104, 1996.
- [3] T. Young, L. Finn, P. E. Peppard, M. Szklo-Coxe, D. Austin, F. J. Nieto, R. Stubbs, and K. M. Hla, "Sleep Disordered Breathing and Mortality: Eighteen-Year Follow-up of the Wisconsin Sleep Cohort," *Sleep*, vol. 31, pp. 1071-1078, 2008.
- [4] T. Young, P. E. Peppard, and D. J. Gottlieb, "Epidemiology of Obstructive Sleep Apnea: A Population Health Perspective," *American Journal of Respiratory and Critical Care Medicine*, vol. 165, pp. 1217-1239, 2002.
- [5] F. Roux, C. D'Ambrosio, and V. Mohsenin, "Sleep-related breathing disorders and cardiovascular disease," *The American Journal of Medicine*, vol. 108, pp. 396-402, 2000.
- [6] J. Quistgaard, "Signal acquisition and processing in medical diagnostic ultrasound," *IEEE Signal Processing Magazine*, vol. 14, pp. 67-74, 1997.
- [7] M. Al-Abed, P. Antich, D. E. Watenpaugh, and K. Behbehani, "Detection of airway occlusion in simulated obstructive sleep apnea/hypopnea using ultrasound: An in vitro study," presented at the 32nd Annual International Conference of the IEEE Engineering in Medicine and Biology Society, Buenos Aires, Argentina, 2010.
- [8] M. Al-Abed, P. Antich, D. E. Watenpaugh, and K. Behbehani, "In vivo characterization of ultrasonic transducers for the detection of airway occlusion in Sleep Disordered Breathing," presented at the 33rd Annual International Conference of the IEEE Engineering in Medicine and Biology Society, Boston, MA, 2011.
- [9] W. R. Hedrick, D. L. Hykes, and D. E. Starchman, *Ultrasound Physics and Instrumentation*, Fourth ed. St. Louis, MO: Elsevier Mosby, 2005.
- [10] A. N. Rama, S. H. Tekwani, and C. A. Kushida, "Sites of Obstruction in Obstructive Sleep Apnea," *Chest*, vol. 122, pp. 1139-1147, 2002.
- [11] R. S. Cobbold, *Foundations of Biomedical Ultrasound*, 1st ed. New York City, New York: Oxford University Press, 2007.
- [12] J. H. Zar, *Biostatistical Analysis*, 4th Edition ed. Upper Saddle River, New Jersey: Prentice hall, 1999.